Analytical Treatment of Neutron-Density Crossplot for Shaly Sand Reservoirs

A.M.K. Basal

Geology Department, Damietta Faculty of Science,
Damietta - 34517, Egypt

Abstract. The neutron-density crossplot represents the basis for analyzing the shaly sand reservoir and coded as SARABAND program. In this paper, a mathematical formulation for obtaining the volume fractions of the three types of shale (laminated, structural and dispersed) is established. The computational sequence involving porosity (Φ) besides the total, laminated and dispersed water saturation calculation models. The effect of light hydrocarbons is also incorporated. The technique depends primarily on the neutron and density logs as shale indicators. This can avoid the use of gamma ray log, hence the confuse with other radioactive elements.

The actual well log data representing the Abu Madi Formation, level III sands in East Baltim-1X and El-Qar'a-2 wells, in addition to the sands of Wakar Formation of Port Fouad marine-3 well were chosen for application. The results obtained revealed a predominance of structural and laminated shales in case of level III sands of the Abu Madi Formation. The simplified laminar water saturation model (SwL) is considered adequate. Wakar sands in Port Fouad marine-3 well, according to the used technique, contain the three types of shale. The total shale model for calculating the water saturation (SwT) is favorable in this case. The production history and the Drill Stem Test (DST) data supported the results obtained and consequently confirmed the validity and accuracy of this technique.

Introduction

One of the best approaches for shaly sand reservoir analysis is the use of neutron-density crossplot (Schlumberger, 1972 and 1974). The graphical separation of the shale volume into the relative amounts of dispersed, laminar and structural is tedious and time consuming. Accordingly, the total shale model of Simandoux (1963) was widely used to calculate the water saturation of the reservoir. This is unfortunate, because the proportions of the shale types may be used as a basis for selecting the proper water saturation of the reservoir. This is unfortunate, because the proportions of the shale types may

be used as a basis for selecting the proper saturation equation. The knowledge of the relative amounts of the various types of shale is useful in any detailed log analysis and in developing exploration models.

The gamma ray log is simultaneously recorded with the neutron and density logs and hence the gamma ray log usually used by the log analysts as a direct shale indicator. However, this shale indicator is not always reasonable (Serra, 1986). In this article, the volume of shale is not extracted from the gamma ray reading, which may be considered as a positive point.

The hydrocarbon correction (if any) can approximated by displacing the actual point in the neutron-density crossplot along a line of constant slope (Poupon *et al.,* 1970). This work tries to conduct this correction by solving non-linear equations and hence to eliminate the human factor and make uses of the computer facilities for enhancing the needed accuracy. Also, the graphical techniques may be a time consuming method for interpretation of a well log data, hence many numbers have to be plotted and treated manually.

Mathematical Treatment of the Neutron-Density Crossplot

Fig. (1) represents the typical frequency crossplot of density (ΦD) and neutron (ΦN) porosities used by Poupon *et al.* (1970). This graphical representation is the basis for the mathematical treatment of the presented model. The cluster of points can be differentiated into three groups (A, B and C). Group "A" represents clean and shaly sands. Group "B" represents shale. Group "C" has a light hydrocarbon effect. The location of "Sho" point can be defined by the lowest ΦD points in group "A" and lowest ΦN points in group "B". The highest ΦN point in group "B" is the west clay "Cl". The "Sho", "Cl", and quartz point "Q" make a straight line "Sd" point has the highest possible crossplot porosity in group "A" and lies on the clean line.

The shale associated with sand can occur in three different types (Schlumberger, 1972). These are structural, dispersed and laminar. When shales exist as grain in the formation matrix, it is called structural. The presence of such type does not effect porosity. In the case, that shale is present in the pores around the sand grains, it is called dispersed. The amount of dispersed shale reduces pore space. Shale may occur as thin layers intercalated in the sand formation and called laminar. Laminar shale replaces both porosity and matrix.

The neutron and density readings from a shale section (ΦNsh and ΦDsh) can define point Sho and hence enables the calculation of the porosity (Φ) and the shale volume (Vsh) for any point plotted on the ΦN-ΦD crossplot. Fig. (2) represents such type of crossplot. The equations expressing the various straight lines are as follows:

Sand line connecting Q(0 , 0) and W (100 , 000)

$$\Phi D = \Phi N \tag{1}$$

Shale line connecting Q(0 , 0), Sho (ΦNsh and ΦDsh) and Cl (ΦNcl and ΦDcl)

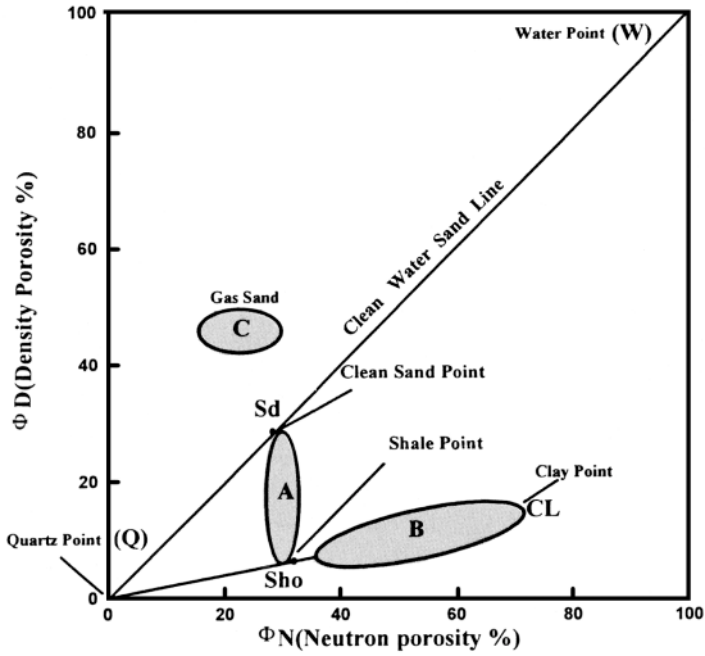$$\Phi D = [\Phi Dsh\ /\ \Phi Nsh]\ \Phi N \tag{2}$$

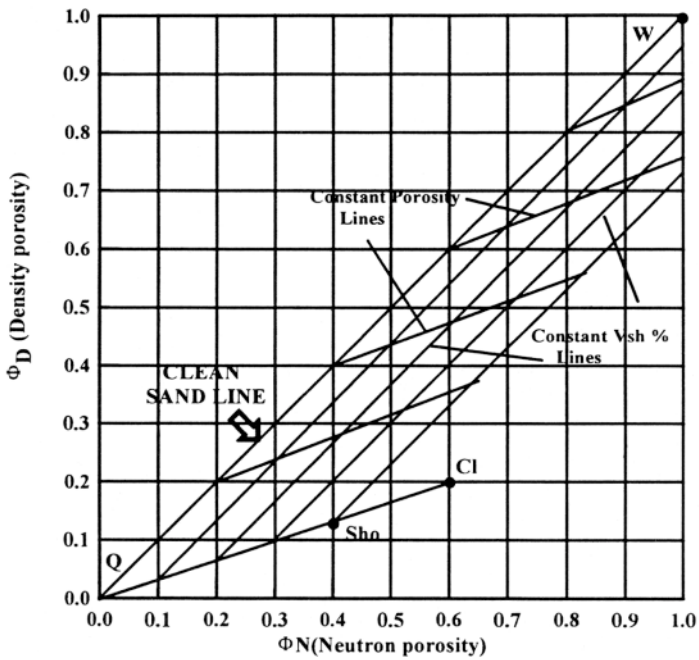FIG. 1. Frequency crossplot of neutron and density of a sand-shale sequence (after Poupon *et al.,* 1970).

FIG. 2. Neutron-density-porosity crossplot used for shaly formation analysis.

Constant porosity lines

$$\Phi D = [\Phi Dsh / \Phi Nsh] \ \Phi N + [1 - \Phi Dsh / \Phi Nsh] \ \Phi \qquad (3)$$

Constant shale lines

$$\Phi D = \Phi N + Vsh \ (\Phi Dsh - \Phi Nsh) \qquad (4)$$

Solving equations (3) and (4) for Φ and Vsh give

$$\Phi = \{ \ \Phi D - [\Phi Dsh / \Phi Nsh] \ \Phi N \ \} / \{1 - [\Phi Dsh / \Phi Nsh]\} \qquad (5)$$

and

$$Vsh = (\Phi D - \Phi N) / (\Phi Dsh - \Phi Nsh) \qquad (6)$$

The above mentioned equations can be applied to water-bearing formations. In formations having light hydrocarbons, correction must be made before applying equations (5) and (6). This correction can be done using the response of porosity logs to shaly formations with hydrocarbons considering the excavation effect. The volume fraction of shale and the corrected porosity in this case can be given by equations (I-6) and (I-9) in Appendix I.

$$Vsh = \Phi D / \Phi Dsh - \{\Phi \ [1 + (1 - Sxo) \ (\Phi Dh - 1)] \ \} / \Phi Dsh \qquad (I - 6)$$

where Sxo is the flushed zone water saturation (fractional) ΦNh and ΦDh are the neutron and density porosities of hydrocarbons which can be calculated, knowing the hydrocarbon density (ρh, gm/cc), using Equations I-3, I-4, and I-5 (Appendix I).

$$\Phi = [-b \pm \sqrt{b^2 - 4ac}] \ / \ 2a \qquad (I-19)$$

where a, b, and c are given by equations I-16, I-17, and I-18 (Appendix I)

The volume fraction of shale (Vsh) can be determined by substituting Φ value into equation I-6. This defines a point on the Φ - Vsh coordinates. The equivalent plot for this point on the ΦN-ΦD crossplot can be determined by setting Sxo = 1 in equations I-1 and I-6 in Appendix I to give

$$\Phi NC = \Phi + \Phi Nsh. \ Vsh \qquad (7)$$

$$\Phi DC = \Phi + \Phi Dsh. \ Vsh. \qquad (8)$$

where: ΦNC and ΦDC represent the corrected neutron and density porosities for the effect of light hydrocarbons.

Volumetric Determination of the Three Types of Shale

The volume fraction of shale (Vsh) obtained in the previous section represents the total shale percent. The Dispersed (VDP), Structural (VS) and Laminated (VL) shales satisfy the following relation:

$$Vsh = VD + VL + VS \qquad (9)$$

Fig. (3) represents the ΦN-ΦD crossplot through which the three shale types can be determined volumetrically. To demonstrate the procedure, the acute axis system Vsh-Φ is transferred into rectangular coordinates, as shown in Fig. (4). Line D represents the trend of dispersed shale. Along this line, point Sd is the clean sand with maximum porosity (Φsd) and VD = 0. Porosity of a clean sand is reduced along this line by adding dispersed shale amounts. The end points for this line is then Φsd (VD = 0) and zero porosity (Vsh = VD). The slope of this line equals unity (Fig. 4), hence it can be expressed mathematically as:
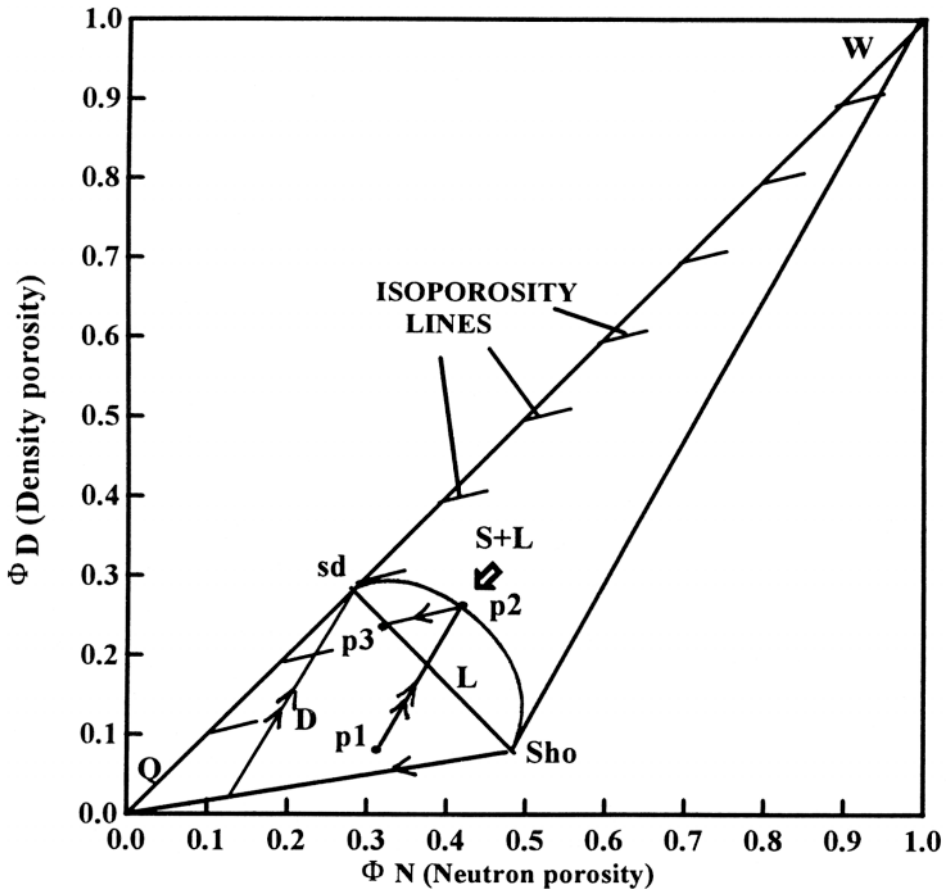

F$_{IG}$. 3. Neutron-density-porosity crossplot, showing the main lines and the displacements for the determination of the amounts of the three types of shale.

$$\Phi = - VD + \Phi sd \qquad (10)$$

Structural and laminar shales can be calculated as an envelop (lumped) of S + L on Fig. 3 (Schlumberger, 1974). This lumped envelop can be expressed as:
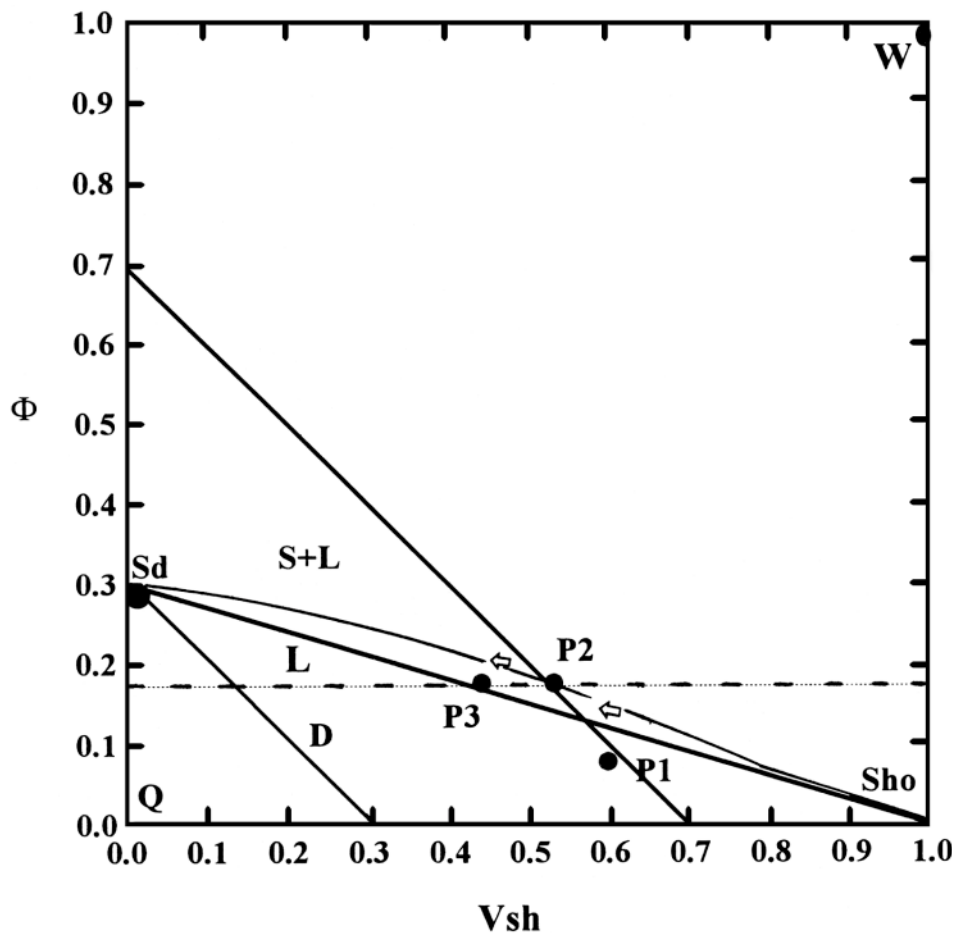
F<small>IG</small>. 4. Shale volume-porosity crossplot, showing the main lines and the displacements for the determination of the amounts of the three types of shale.

$$\Phi = \Phi\text{sd} \, (\text{VS} + \text{VL})^3 - 2.\Phi\text{sd} \, (\text{VS} + \text{VL})^2 + \Phi\text{sd} \tag{11}$$

The laminar shale line (line L on Figs. 3 and 4) can be formulated as:

$$\Phi = -\Phi\text{sd}. \, \text{VL} + \Phi\text{sd} \tag{12}$$

All shaly sands after the correlation of the hydrocarbon effect should fall in the region bounded by Line D and curve S + L.

Two displacement have to be conducted. First, Point P1 (arbitrary chosen) of co-ordinates (Φ1 and Vsh1) must be displaced into point P2 along a line parallel to line D, that pass through point PL until intersecting the S + L envelop (Fig. 4). This will eliminate the effect of dispersed shale and hence the remaining are structural and laminar shales. This will locate point P2 with coordinates (Vsh2 and Φ2). Line P1P2 has the relation:

$$\Phi = - \text{Vsh} + \Phi 1 + \text{Vsh1} \tag{13}$$

The volume of structural and laminar shales (VS + VL) is equal to Vsh2 and can be determined by solving equations (11) and (13) as: (Equation II-31 in Appendix II)

$$\text{Vsh2} = \sqrt[3]{R + \sqrt{U}} \; - \; \sqrt[3]{|R - \sqrt{U}|} \; + \; 2/3 \tag{II - 31}$$

where:
$$R = \frac{1}{\Phi \text{sd}} \left[\frac{\Phi 1 + \text{Vsh1}}{2} \right] - \frac{11}{54} \tag{II - 15}$$

$$U = R^2 + \left(-\frac{4}{9} + \frac{1}{3\Phi \text{sd}} \right)^3 \tag{II - 29}$$

Obtaining Vsh2 and substituting this value into equation (13) gives:

$$\Phi 2 = - \text{Vsh2} + \Phi 1 + \text{Vsh1} \tag{14}$$

The second displacement is done along a constant porosity line passing through point P2 (Fig. 4) whose equation is:

$$\Phi = \Phi 2 \tag{15}$$

The intersection of this line with the laminar shale line L determines point P3 with coordinates ($\Phi 3$ and Fsh3). Vsh3 represents the volume fraction of laminar shale and can be given as:

$$\Phi 3 = \Phi 2 = - \Phi \text{sd. VL} + \Phi \text{sd} \tag{16}$$

where VL = Vsh 3

$$\text{VL} = 1 - (\Phi 2 / \Phi \text{sd}) \tag{17}$$

The volume fraction of structural shale is

$$\text{VS} = (\text{VS} + \text{VL}) - \text{VL} = \text{Vsh2} - \text{Vsh3} \tag{18}$$

The dispersed shale value is given as:

$$\text{VD} = \text{Vsh1} - \text{Vsh2} \tag{19}$$

Water Saturation Calculation Models

If the shale present in the formation is predominantly dispersed, the following equation (de Witte, 1950) can be used:

$$\text{SWD} = \frac{\sqrt{\dfrac{\text{aRw}}{\text{RT.}\phi \text{im}^2} + \dfrac{q^2}{4}} - \dfrac{q}{2}}{1 - q} \tag{20}$$

where: q = Vd / Φim and Φim = Φ + VD

If the shale is predominantly structural and laminar, the laminated shale simplified equation (Poupon *et al.,* 1954) can be used as:

$$SwL \ = \ \sqrt{\left[\frac{1}{R_t} - \frac{V_{lam}}{R_{sh}}\right] \cdot \left[\frac{aR_w(1 - V_{lam})}{\phi^2}\right]} \tag{21}$$

where: V_{lam} equals the volume fraction of both laminated and structural shales (VL + VS).

In case, when the shale type can not be determined, Simandoux (1963) proposed the total shale model is:

$$SwT \ = \ \frac{\dfrac{-Vsh}{Rsh} + \sqrt{\left(\dfrac{Vsh}{Rsh}\right)^2 + \dfrac{4\Phi^2}{aRw.RT(1-Vsh)}}}{\dfrac{2\Phi^2}{aRw(1-Vsh)}} \tag{22}$$

The flow chart for the program representing the previously discussed sequence is presented in Fig. (5).

Illustrative Example

It is important here to mentioned that, this technique can be applied to reservoirs containing the various types of shales (dispersed, laminar and structural), in addition to the light hydrocarbons, if present. The following illustrative example demonstrates the procedure and the way of treating the well log data. Five points representing the various probable situations, which may exist, were proposed. The ΦN = ΦD crossplot for these points is shown in Fig. (6). Point 1 lies on the dispersed shale line. Points 2 and 3 are expected to contain the three types of shales. Point 4 is chosen on the structural and laminar shale envelop. The effect of light hydrocarbons (gas) is seen as point 5. Arrows in Figs. 6 and 7 show graphically the displacements required, as mentioned early. For point 2, a line is drawn parallel to the dispersed shale line until it intersects the structural and laminar shales envelop. This intersection point defines the amount of VS + VL, since VD = 0. For this new point, VS + VL is 0.23 and VD = 0.33 - 0.23 or VD = 0.1. A line is drawn from that point on the VS + VL envelop to the L line following a path of constant porosity. The intersection defines the VL and is equal to 0.09 and then VS = 0.23 - 0.09 = 0.14.

Point 3 (Figs. 6 and 7) agrees with the physical observations, since sands with laminar shale generally contain dispersed and structural types (Desbrandes, 1985). For point 4, the value of Φ, as deduced from this crossplot (Fig. 6), is 0.15 and that of Vsh is 0.6. Point 5 that plotted above the clean sand line has to be corrected for the effect of gas. Point 5′ represents the corrected equivalence for this point. Then the procedure is conducted for point 5′ as mentioned above.

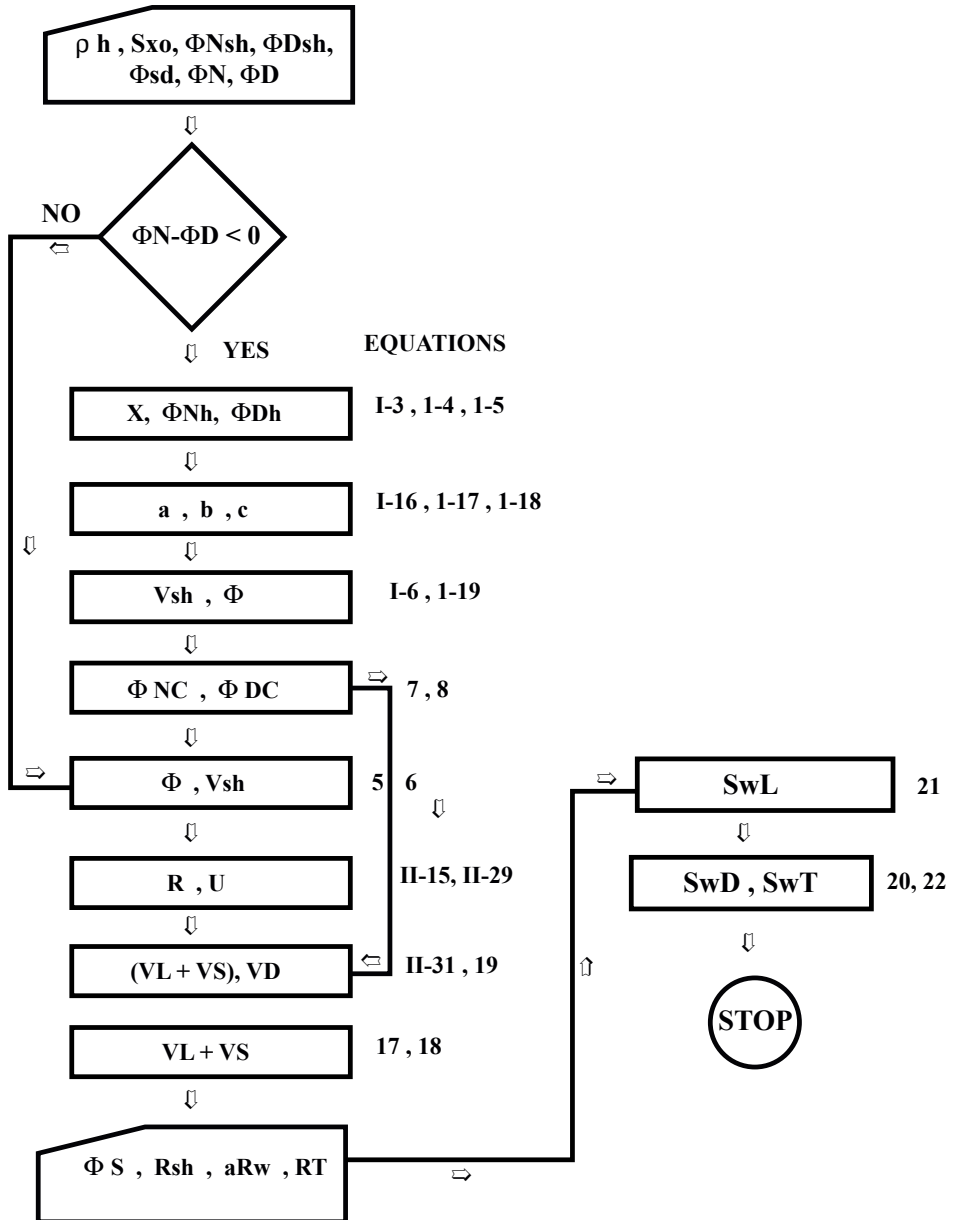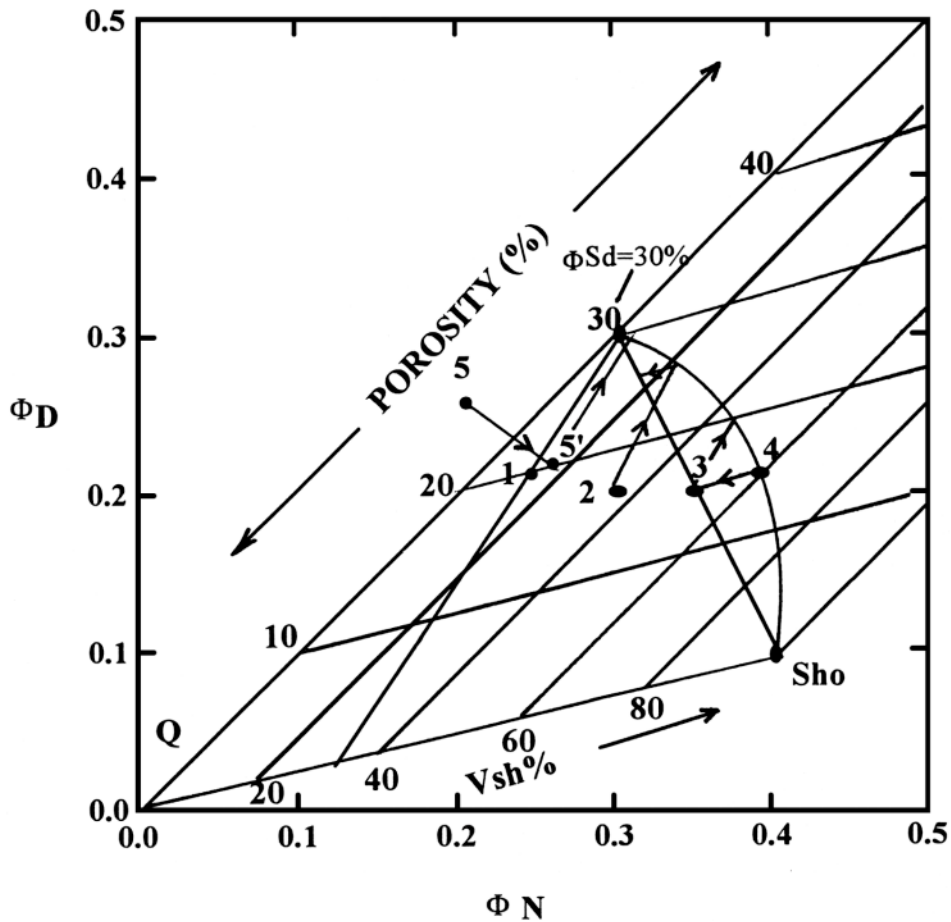FIG. 5. Flow chart representing the calculations for the applied technique.

FIG. 6. Data points of example "1" on the ΦN-ΦD crossplot, showing the displacements for determining the volume of the three types of shale.
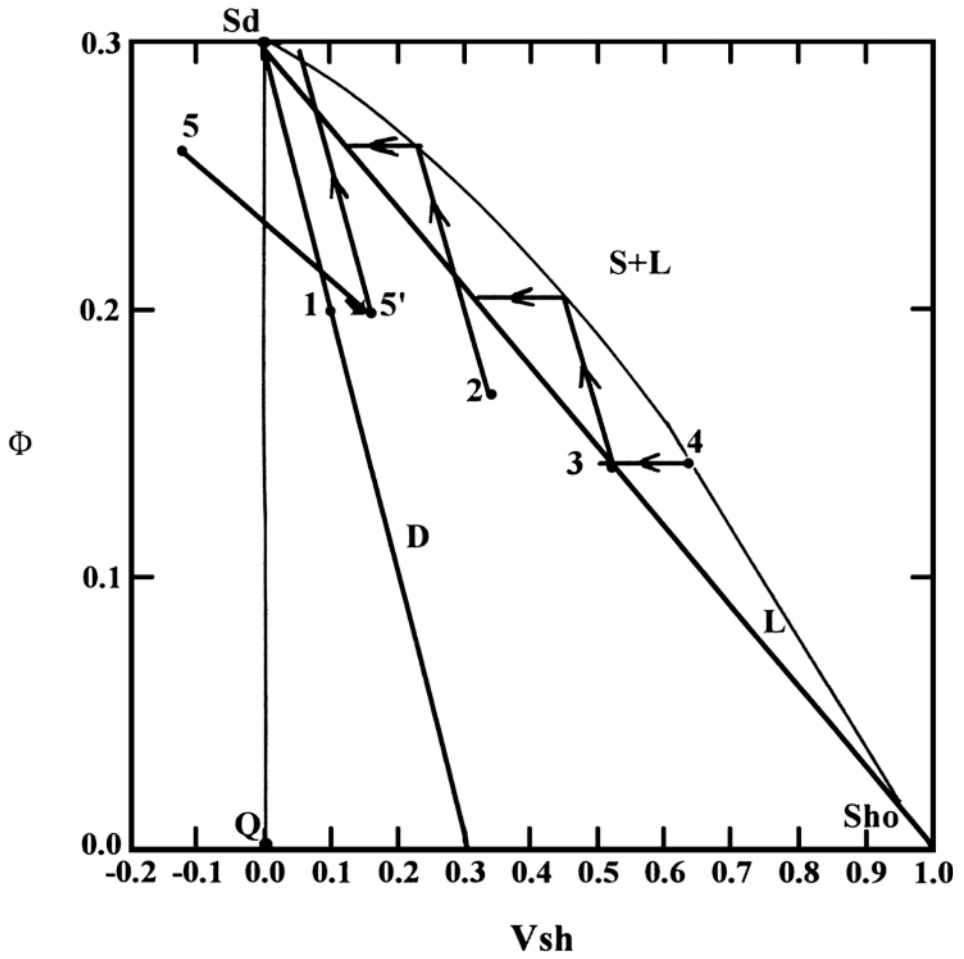
F<small>IG</small>. 7. Data points of example "1" on the Vsh - F crossplot, showing the displacements for determination of the three types of shale.

The proposed well log values for the above mentioned five points and the results obtained by applying the presented analytical treatment are represented in Table (1). The following parameters also assumed, these are: $\Phi sd = 0.3$, $\rho h = 0.3$ gm/cc, $aRw = 0.1$, $Sxo = 0.6$, $\Phi Nsh = 0.4$, $\Phi Dsh = 0.1$ and $Rsh = 6.5 \, \Omega m$.

TABLE 1. The input well log data and the output results for the proposed five points illustrating the way of analytical treatment presented.

Point	ΦN %	ΦD %	ΦS %	Rt Ωm	Φ %	Vsh %	VD %	VS %	VL %	SwT %	SwD %	SwL %
1	24	21	23	15	20	10	10	0.0	0.0	37	34	–
2	30	20	25	8	17	33	10	13	10	42	45	49
3	35	20	30	6	15	50	6	14	30	53	44	49
4	39	21	30	5	15	60	0.0	10	50	52	49	44
5	21	25	23	7	20	12	9	0.0	3	54	52	58

If points 1 to 4 have also light hydrocarbon, the presence of shale will mask the effect on both neutron and density readings. Table (2) represents the results obtained in this case, if the zones assumed to have gas.

TABLE 2. The different shale type volumes and the corresponding water saturations obtained in case of the presence of light hydrocarbons.

Point	Φ%	Vsh %	VD %	VS %	VL %	SwT %	SwL %	SwD %
1	15	31	13.4	12.6	5	42	38	26
2	12	57	7	13	37	49	41	68
3	11	69	25	44	0.0	53	46	50
4	11	79	30	49	0.0	54	72	50

Application

In this respect, three gas wells were chosen for the application of such a presented systematic approach. These are Abu Madi Formation (level III) in East Baltim-1X and El-Qar'a-2 wells, as well as Wakar Formation in Port Fouad marine-3 well (Fig. 8). The following sections represent a treatment for the sands of Abu Madi and Wakar Formations in these wells.

1-Abu Madi Formation, Level III [East Baltim - 1X, (Jh 63-1) Well]

Two gas bearing sand levels were identified within the Abu Madi Formation of Messinian age, designated as levels II and III. Level 1 sands was found water bearing (El-Heiny *et al.,* 1990). East Baltim-1x is the first commitment well to be drilled in the Baltim offshore concession. The area was acquired by IEOC and AMOCO in 1992. The major reservoir bodies are represented by sandstone, mainly fluvial and developed in the active channel belts as a response to the relative fall of the sea level. Fig. (9) represents a log suite for East Baltim-1 (Jh63-1) well, showing Abu Madi sand level III. This well is considered as gas and condensate well. The Drill Stem Test (DST) data revealed gas production rate of 31.5 MMSCF/D and condensate with rate of 639 BCPD
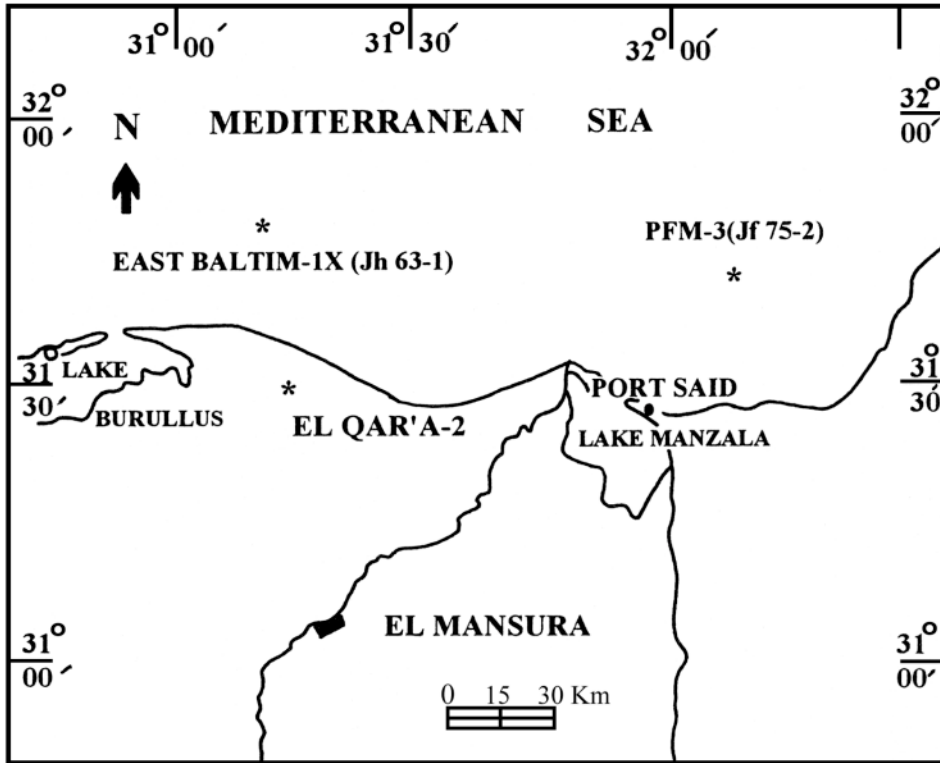
FIG. 8. Location map for the three studied gas wells.

(E.G.P.C., 1994). The ΦN-ΦD crossplot for 12 selected intervals is represented in Fig. (10). The points plotted below this line indicate shale effect. Point D represents a shale point (ΦNsh = 0.4 and ΦDsh = 0.03). The 100% clean water bearing sand is represented by point 12 and has (Φsd) equals 0.20. The parameters used are: ΦNsh = 0.4, ΦDsh = 0.03 (point 9), Sxo = 0.6 and Φsd = 0.2. The well log data and the results obtained are summarized in Table (3).

The results obtained in the table above clearly indicate that, the structural and laminar types of shale are predominant. Accordingly, the simplified laminated water saturation model (SwL) is adequate in such a case. The (RT) tool is not available, hence the water saturation models can not be calculated.

2 - Abu Madi Formation, Level III [EL Qar'a-2 Well]

Fig. (11) represents the available well log suite for level III in this well. Twelve points were selected. The ΦN = ΦD crossplot for these points is seen in Fig. (12). The parameters used are: ρh = 0.4 gm/cc, Sxo = 0.5, ΦNsh = 0.35, ΦDsh = 0.05, Φsd = 0.19, Rsh = 0.8 Ωm and aRw = 0.28. The input well log data and the deduced results are presented in Table (4).
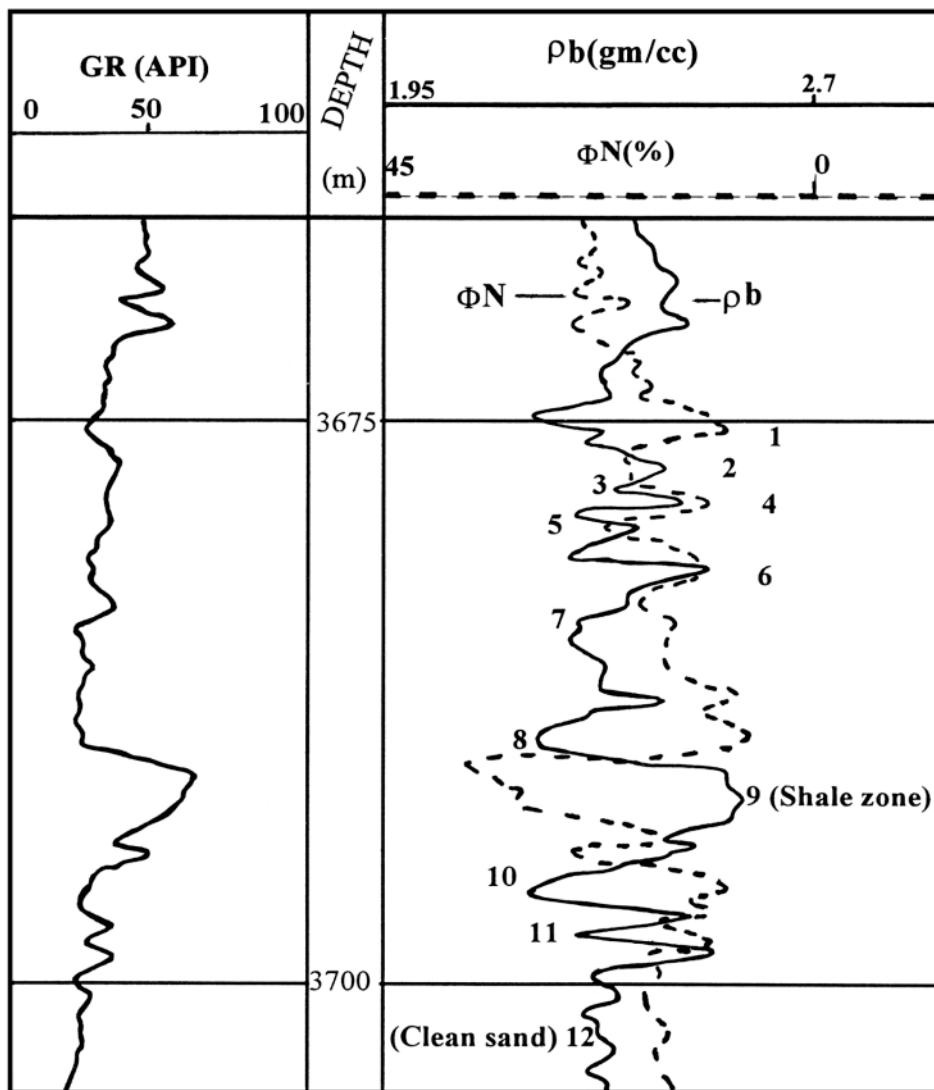
F<small>IG</small>. 9. Well log suite of Abu Madi Formation (Level III) in East Baltim-1X (Jh 63-1) well, north Nile Delta, Egypt (E.G.P.C., 1994).
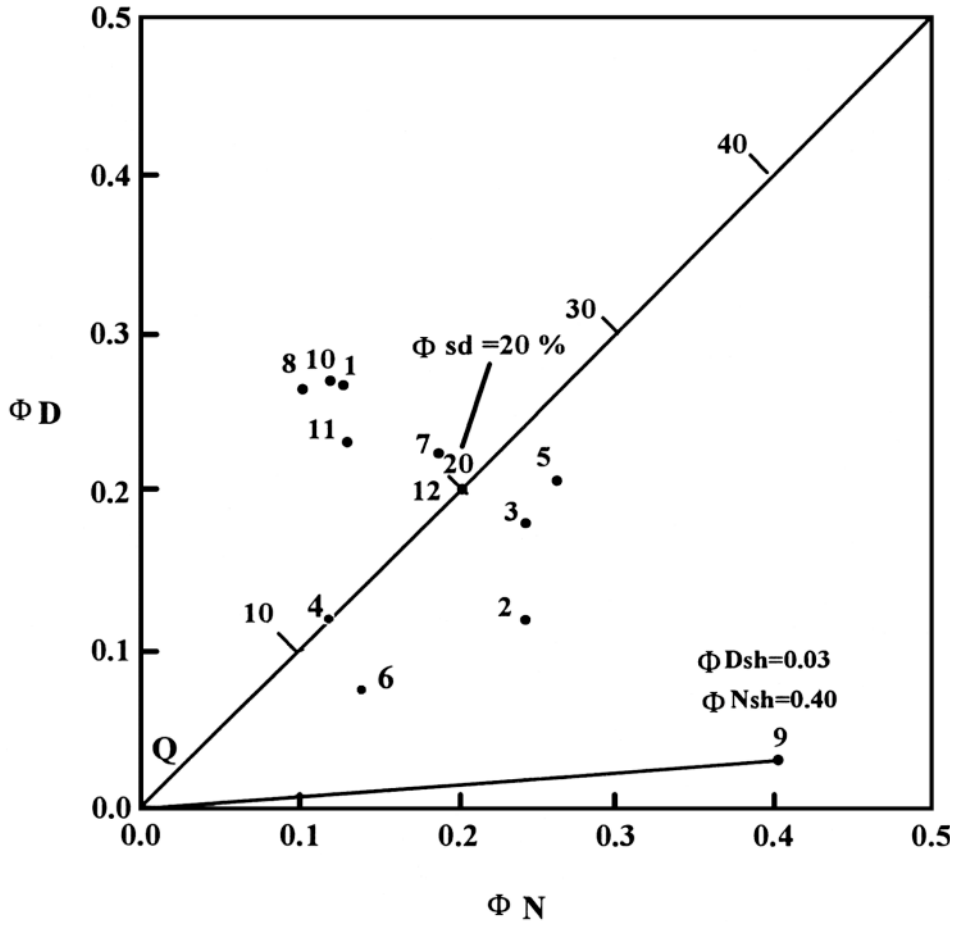
F<small>IG</small>. 10. FN-FD Crossplot for Abu Madi Gas bearing sand (Level III), East Baltim-1X (Jh 63-1) well, north Nile Delta, Egypt.

TABLE 3. The input well log data and the output results for Abu Madi Formation, Level III in East Batim-1X, (Jh63-1) well, Nile Delta.

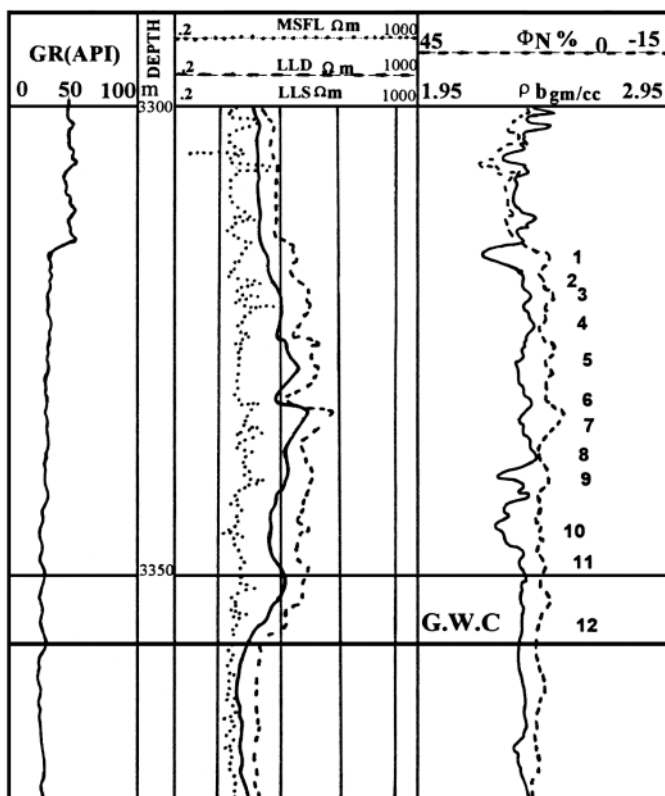| Zone	ρbgm / cc	ΦN%	ΦD %	Φ %	Vsh %	VL %	VS %	VD %
1	2.2	13	27	22	5	0	5	0
2	2.45	24	12	9	34	10	15	9
3	2.35	24	18	14	31	10	17	4
4	2.47	12	11	9	- ve	–	–	–
5	2.3	26	21	16	49	20	29	0
6	2.53	14	7	5	29	0	21	8
7	2.27	18.5	23	18	35	10	25	0
8	2.21	10	27	22	5	0	5	0
9	2.6	40	3	40	100		**Shale**	**Zone**
10	2.2	11.5	27	22	5	0	5	0
11	2.25	13.5	24	19	27	5	24	0
12	2.32	20	20	20	0.00	**Clean**	**Sand**	**Zone**

FIG. 11. Well log suite for Abu Madi formation (Level III) in El Qara'2 well, Nile Delta, Egypt (E.G.P.C., 1994).

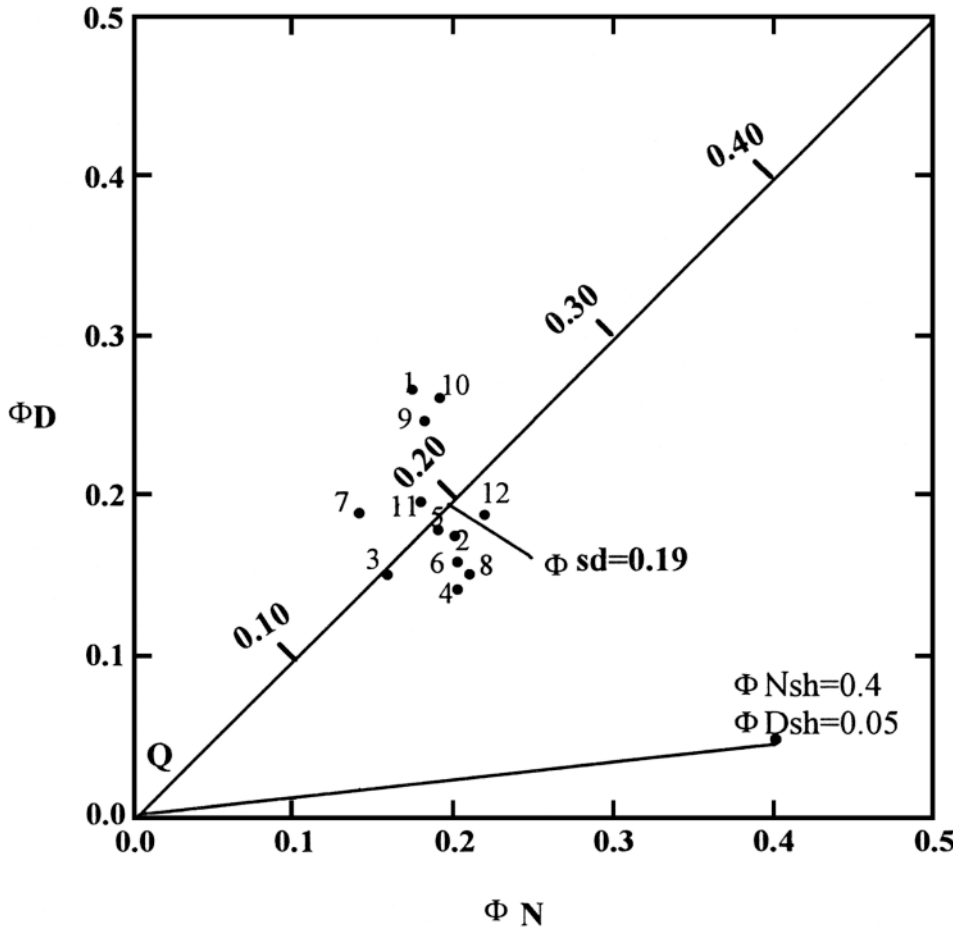Fɪɢ. 12. ΦN-ΦD crossplot for Abu Madi Formation (Level III) in El Qar'a-2 well, Nile Delta, Egypt.

TABLE 4. The input well log data and the output results for Abu Madi Formation, Level III in El Qar'a-2 well, Nile Delta.

Zone	ρb gm/cc	ΦN %	ΦD %	RT Ωm	Φ %	Vsh %	VS %	VL %	VD %	SwT %	SwL %	SwD %
1	2.19	17	29.6	20	23	3	3	0	0	49	48	–
2	2.37	20	18	15	13	27	17	5	5	71	60	87
3	2.41	16	15.5	30	11	28	5	16	7	50	22	60
4	2.43	20	14	20	10	24	15	0	9	75	65	81
5	2.37	19	18	30	14.5	12	6.7	1	4.3	54	46	53
6	2.42	20	15	10	11	18	10	0	8	100	100	100
7	2.35	14	19	80	15	– ve	Clean	Sand	Zone			
8	2.41	21	15.5	23	11	28	16	5	7	58	40	73
9	2.27	18	24.5	35	19	4	0	4	0	45	42	–
10	2.25	19	26	35	20	8	8	0	0	40	35	–
11	2.35	18	19	32	14	21	13.9	2.6	4.5	45	24	52
12	2.35	21	19	10	14	22	13.9	2.6	4.5	91	88	100

The careful examination for the tabulated results clearly indicates that, the structural and laminated shale types are the major proportions in the sands of East Baltim-1X well, as mentioned above. It is important here to mention that, the negative values for the Vsh (zone 7) indicate that, the technique is valid only in case of shaly sands and this zone is clean (Vsh = 0). The most important and interesting point is that, the water saturation using the laminar model (SwL) gave the lowest values, which match with the fact that, this is a gas producing sand (E.G.P.C., 1994). The total shale model (SwT) gave values exceptionally higher than those of the laminar one (zones 3 and 11). On the other hand, the dispersed shale model (SwD) gave unrealistic values for such producing reservoir (more than 52% and sometimes reach 87%).

3 – *Wakar Formation [Port Fouad Marine-3 (Jf 75-2) Well]*

Port Fouad Marine gas field is located in the North Port Said concession of the IEOC, approximately 35 Km northeast of Port Said (Fig. 8). Well Port Fouad marine-3, PFM-3 (Jf75-2) was drilled in 1992 to a total depth of 10404 feet as a gas and condensate discovery (E.G.P.C., 1994). Four main gas bearing intervals were discovered (S0, S1, S2 and S3). These levels are present in PFM-3 (Jf 75-2) well. This well produces from the Wakar Formation (Tortonian). The gas sands of this formation is mainly composed of quartz metamorphic, volcanic fragments and cherts occur in silty-shaly fossiliferous section (E.G.P.C., 1994). The production is mainly from two levels, Upper and Lower. The Upper level produces 26 MMSCFG/D & 1262 BC/D of 51º API. The Lower level produces 34 MMSCFG/D & 1609 BC/D of 50º API. (Fig. (13)) represents the available well log suite for PFM-3 (JF75-2) well. The first glance for the neutron and density logs
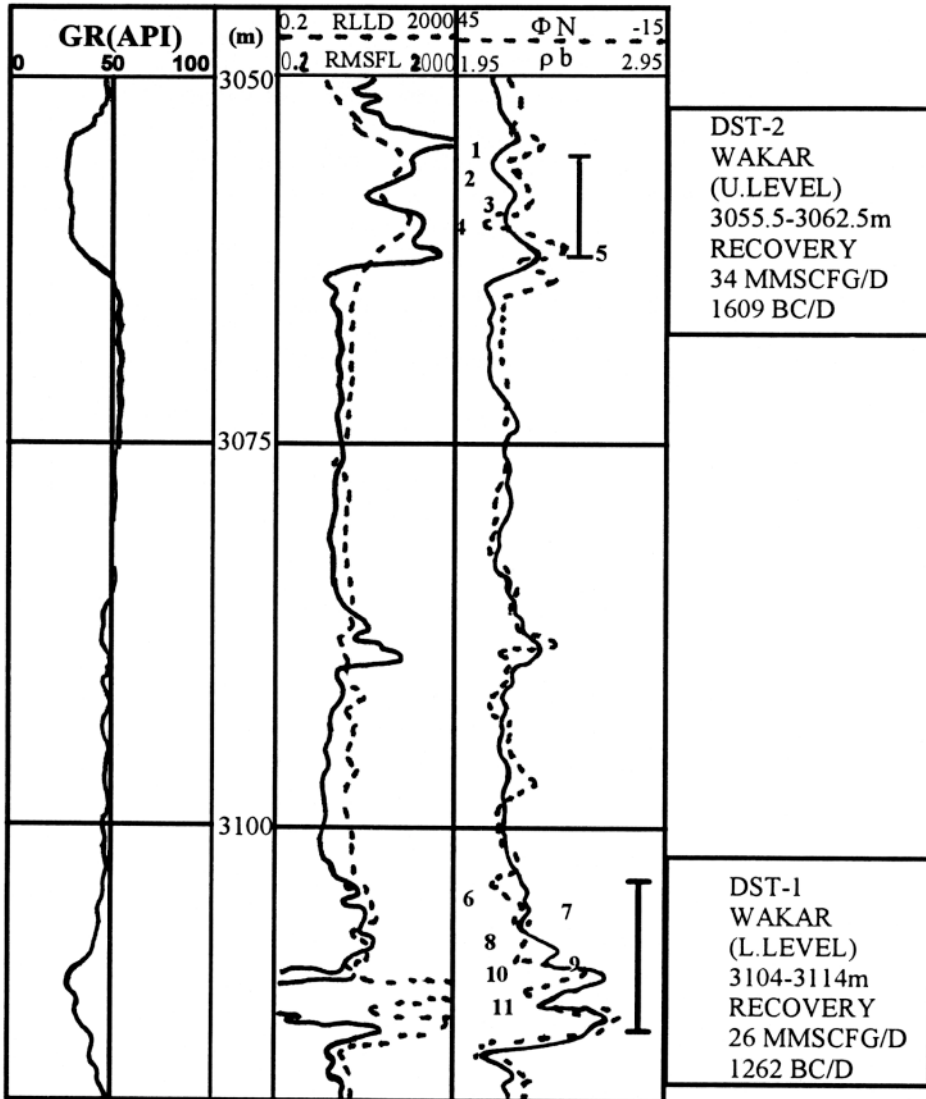
F<small>IG</small>. 13. Well log suite for Wakar Formation (Upper Miocene) in PFM-3 (Jf 75-2) well, North Sinai, Egypt (E.G.P.C., 1994).

do not reflect by any mean the presence of gas (no gas crossover is seen). The presence of shale masked the gas effect on both the neutron and density curves. The ΦN-ΦD crossplot for some selected intervals is shown in Fig. (14). It is clear from this plot that, the points plotted below or near the clear sand line do not reflect any gas effect (gas normally shifts the plotted points toward the northwest direction above the clean sand line). The following values are used: ρh = 0.2 gm/cc, aRw = 0.28, Rsh = 8Ωm, ΦNsh = 0.35, ΦDsh = 0.11 and Sxo = 0.7. Table (5) represents the input well log data and the output results obtained using the presented technique, taking into account the presence of gas. It is clear from the results obtained that, the lower level, generally, has shale content more than that of the upper level. Also, the upper has higher porosity (Φ). Zones 2 and 5 have negative Vsh, which indicate clean zones, as mentioned early. The lower level contains the three types of shale and consequently, the total shale model is valid in such a situation. The shaly zones in the upper level contain structural and dispersed shales, which also indicate the validity of the total shale model. The water saturations are presented in Table (6). The water saturation results clearly indicate that, the Upper level has lower water saturation (SwT) than the Lower level. The Drill Stem Test (DST) results for this well (E.G.P.C., 1994) are as follows :

Φe: 20-30%   **Upper Level**
Sw: 45-60%

Φe: 8-23%   **Lower Level**
Sw: 76%

As shown, the (DST) results support the conclusions obtained through such a technique.

Summary and Conclusions

The mathematical formulation for the neutron-density graphical representation was conducted through a series of equations. These equations can calculate porosity, total bulk volume fraction of shale, and the relative amounts of laminated, structural and dispersed shale types. The gamma ray log is excluded as a shale indicator to avoid any confusion with the other radioactive minerals not related to the presence of shales. The water saturation model can be chosen according to the predominant shale type. These models are: total shale (SwT), simplified laminated (SwL) and dispersed (SwD). A theoretical model was provided to demonstrate the procedure and the computational sequence.

Two gas producing sand occurrences were chosen for application. The first is in Abu Madi sand, level III in East Baltim-1X, (Jh63-1) and El Qara'a 2 Wells in the Nile Delta province. The second is in Wakar sand in Port Fouad Marine-3 (Jf 75-2) well in North Sinai province. The obtained results indicated the predominance of both the laminated and structural shale types for Abu Madi sand, level III in both wells and the three types of shales in Wakar sand. Accordingly, a simplified laminated shale water saturation model (SwL) was suggested for the Abu Madi sand, while the total shale water saturation model (SwT) was proposed for the Wakar sand. The production history and the Drill Stem Test (DST) data supported the deduced results.
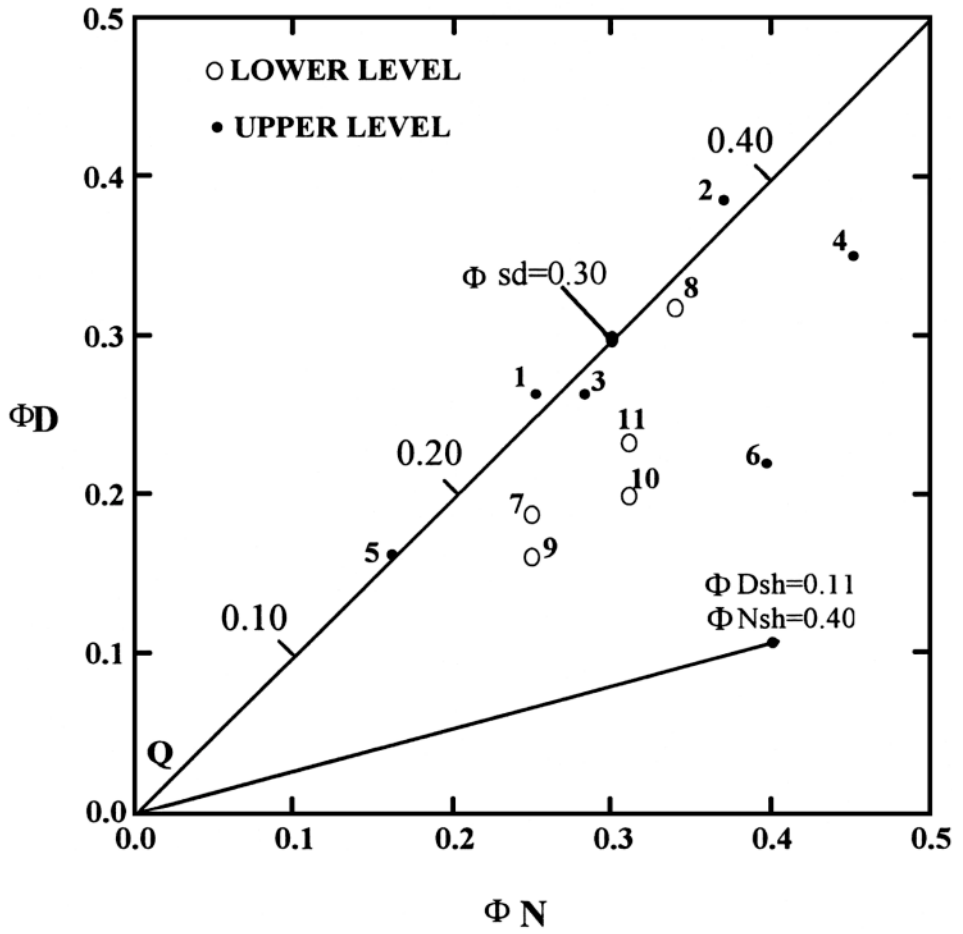
F<small>IG</small>. 14. FN-FN crossplot for Wakar Gas bearing sands (upper and lower levels) in PFM-3 (Jf 75-2) well, North Sinai (Egypt).

TABLE 5. The input well log data and the output results for Wakar Formation in Port Fouad Marine-3 (Jf 75-2) well, Nile Delta.

Zone	ρbg/cc	ΦN %	ΦD %	RT Ω m	Φ %	Vsh %	VL %	VS %	VD %	Level
1	2.25	25	26	27	20	18	0	8	10	upper
2	2.06	37	38	30	32	**– ve**	0	0	0	upper
3	2.24	28	26	19	25	7	0	7	0	upper
4	2.07	45	37	40	23	86	–	–	–	upper
5	2.4	16	16	20	16	**– ve**	0	0	0	upper
6	2.3	40	22	19	15	62	–	–	–	lower
7	2.35	25	19	23	17	21	0	8	13	lower
8	2.15	34	32	8	23	39	23	16	0	lower
9	2.4	25	16	18	12.6	31	3	11.5	16.5	lower
10	2.34	31	20	8	16	38	17	12	9	lower
11	2.29	31	23	11	15	45	23	14	8	lower

Table 6. Calculated water saturations for various shale types for Wakar Formation Port Fouad Marine-3 (Jf 75-2) well, Nile Delta.

Zone	VL %	VS %	VD %	SwT %	SwL %	SwD %	Level
1	0	8	10	40	29	31	upper
2	Clean	sand					upper
3	0	7	0	45	43	–	upper
4	**Shale**	**Zone**					upper
5	**Clean**	**Sand**	**Zone**				upper
6	**Shale**	**Zone**					lower
7	0	8	13	50	36	37	lower
8	23	16	0	56	49	–	lower
9	3	11.5	16.5	61	45	53	lower
10	17	12	9	78	73	92	lower
11	23	14	8	61	49	83	lower

Appendix I

Hydrocarbon Correction in Shaly Formations

The response equations of neutron and density porosities for shaly formations containing hydrocarbons, considering the excavation effect, are given by Poupon *et al.* (1970) as follows:

$$\Phi N = \Phi + \Phi Nsh. \, Vsh + \Phi(1 - Sxo)(\Phi Nh - 1)(1 + 2\Phi Sxo) \qquad (I-1)$$

$$\Phi D = \Phi + \Phi Dsh. \, Vsh + \Phi(1 - Sxo)(\Phi Dh - 1) \qquad (I-2)$$

where: ΦNh and ΦDh can be calculated, knowing the hydrocarbon density (ρh, gm/cc), as follows:

$$x = 4 - 2.5 \, \rho h \qquad (I-3)$$

$$\Phi Nh = \{9 \, x / (12 + \rho h)\} \qquad (1-4)$$

$$\Phi Dh = \frac{12}{7} - \frac{9}{7} \left\{ \frac{(6+x)}{(12+x)} \right\} \rho h \qquad (I-5)$$

Solving equations I – 1 and I – 2 for Vsh gives:

$$Vsh = \Phi D / \Phi Dsh - \{\Phi[1 + (1 - Sxo)(\Phi Dh - 1)]\} / \Phi Dsh \qquad (I-6)$$

Substituting equation I-6 in equation I-1 to obtain a polynomial in terms of Φ as:

$$\Phi N = \Phi + \frac{\Phi Nsh}{\Phi Dsh} \Phi D - \frac{\Phi(\Phi Nsh)[1 + (1 - Sxo)(\Phi Dh - 1)]}{\Phi Dsh} + \Phi(1 - Sxo)(\Phi Nh - 1)(1 + 2\Phi Sxo) \qquad (I-7)$$

$$\left[\frac{\Phi Nsh}{\Phi Dsh} \Phi D - \Phi N \right] + \Phi - \frac{\Phi(\Phi Nsh)[1 + (1 - Sxo)(\Phi Dh - 1)]}{\Phi Dsh} + \Phi(1 - Sxo)(\Phi Nh - 1)(1 + 2\Phi Sxo) = 0 \qquad (I-8)$$

$$X + \Phi - \Phi \frac{\Phi Nsh}{\Phi Dsh} Y + \Phi.Z(1 + 2\Phi Sxo) = 0 \qquad (I-9)$$

where : $X = \dfrac{\Phi Nsh}{\Phi Dsh} \Phi D - \Phi N$

$Y = [1 + (1 - Sxo)(\Phi Dh - 1)]$

$Z = (1 - Sxo)(\Phi Nh - 1)$

$$\Phi Z(1 + 2\Phi Sxo) + \Phi - \Phi \frac{\Phi Nsh}{\Phi Dsh} Y + X = 0 \qquad (I-10)$$

$$\Phi Z + 2.\Phi^2.Z.Sxo + \Phi \left[1 - \frac{\Phi Nsh}{\Phi Dsh} Y \right] + \frac{\Phi Nsh}{\Phi Dsh} \Phi D - \Phi N = 0 \qquad (I-11)$$

$$2\Phi^2 \, Sxo \, (1 - Sxo)(\Phi Nh - 1) + \Phi + \Phi Z - \Phi \frac{\Phi Nsh}{\Phi Dsh} Y + \frac{\Phi Nsh}{\Phi Dsh} \Phi D - \Phi N = 0 \qquad (I-12)$$

$$2\Phi^2 \, Sxo \, (1 - Sxo)(\Phi Nh - 1) + \Phi \{1 + Z - \frac{\Phi Nsh}{\Phi Dsh} Y\} + \frac{\Phi Nsh}{\Phi Dsh} \Phi D - \Phi N = 0 \qquad (I-13)$$

A.M.K. Basal

$$\Phi^2.2\,Sxo\,(1-Sxo)(\Phi Nh-1)+\Phi\{1+(1-Sxo)(\Phi Nh-1)-\Phi Nsh/\Phi Dsh[1+(1-Sxo)(\Phi Dh-1)]\}+$$

$$(I-14)$$

$$+\,(\Phi Nsh/\Phi Dsh).\Phi D-\Phi N=0$$

This is a quadratic equation in the form:

$$\Phi^2\,a+\Phi b+C=0 \qquad\qquad (I-15)$$

where: $a=2Sxo\,(1-Sxo)\,(\Phi Nh-1)$ $\qquad\qquad (I-16)$

$\qquad b=1+(1-Sxo)\,(\Phi Nh-1)-\Phi Nh/\Phi Dsh\,[1+(1-Sxo)\,(\Phi Dh-1)]$ $\qquad (1-17)$

$\qquad c=[\Phi Nsh/\Phi Dsh]\,.\,\Phi D-\Phi N$ $\qquad\qquad (I-18)$

when solved for Φ gives:

$$\Phi\ =\ [-b\pm\sqrt{b^2-4ac}\ /\ 2a \qquad\qquad (I-19)$$

Equation I-19 will give two values for Φ, accordingly, the real values only (positive) will be considered.

Appendix II

Determination of the volume fractions of Laminar and Structural shales (Vsh2). The equations used are:

$$\Phi\ =\ \Phi sd\,(Vsh2)^3-2\,\Phi sd\,(Vsh2)^2+\Phi sd \qquad\qquad (11)$$

$$\Phi\ =\ -Vsh2+\Phi 1+Vsh1 \qquad\qquad (13)$$

dividing the two equations by Φsd and rearranging can give:

$$(Vsh2)^3-2\,(Vsh2)^2+1\ =\ \frac{-Vsh2}{\Phi sd}+\frac{\Phi 1+Vsh1}{\Phi sd} \qquad\qquad (II-1)$$

$$(Vsh2)^3-2\,(Vsh2)^2+1+\frac{Vsh2}{\Phi sd}-\frac{\Phi 1+Vsh1}{\Phi sd}\ =\ 0 \qquad\qquad (II-2)$$

$$(Vsh2)^3-2\,(Vsh2)^2+\frac{1}{\Phi sd}\,Vsh2+\left(1-\frac{\Phi 1+Vsh1}{\Phi sd}\right)\ =\ 0 \qquad\qquad (II-3)$$

Equation II-3 is a cubic Equation in the form

$$Y^3+a_1\,Y^2+b\,Y+C=0 \qquad\qquad (II-4)$$

where: $a_1=-2$ $\qquad\qquad (II-5)$

$$b\ =\ \frac{1}{\Phi sd} \qquad\qquad (II-6)$$

$$C\ =\ \frac{\Phi sd-(\Phi 1+Vsh1)}{\Phi sd} \qquad\qquad (II-7)$$

Accordingly, equation II-3 becomes:

$$(Vsh2)^3+a_1.\,(Vsh2)^2+b.Vsh^2+C=0 \qquad\qquad (II-8)$$

This equation can be written as:

$$(X - \frac{a_1}{3})^3 + a_1 (X - \frac{a_1}{3})^2 + b (X - \frac{a_1}{3}) + C = 0 \qquad \text{(II – 9)}$$

where : $Vsh2 = X - \frac{a_1}{3}$ \qquad (II – 10)

Solving equation II – 9 gives:

$$X^3 + 3 X^2 (-\frac{a_1}{3}) + 3X (-\frac{a_1}{3})^2 + (-\frac{a_1}{3})^3 + al (X^2 - \frac{2a_1}{3} X + \frac{a_1^2}{9}) + b(X - \frac{a_1}{3}) + C = 0 \qquad \text{(II – 11)}$$

$$X^3 + (\frac{-a_1^2}{3} + b) X + \frac{2a_1^3}{27} - \frac{ba_1}{3} + C) = 0 \qquad \text{(II – 12)}$$

This equation can be written as:

$$X^3 + P.X - 2 R = 0 \qquad \text{(II – 13)}$$

where : $P = \frac{-a_1^2}{3} + b$

$$= -\frac{4}{3} + \frac{1}{\Phi sd} \qquad \text{(II – 14)}$$

$$R = \frac{-a_1^3}{27} + \frac{ba_1}{6} - \frac{C}{2}$$

$$= \frac{8}{27} - \frac{1}{3\Phi sd} - \frac{[\Phi sd - (\Phi 1 + Vsh1)]}{2\Phi sd}$$

$$= \frac{1}{\Phi sd} \left[-\frac{1}{3} + \frac{1}{2} (\Phi 1 + Vsh1) \right] + \frac{8}{27} - \frac{1}{2}$$

$$= \frac{1}{\Phi sd} \left[\frac{\Phi 1 + Vsh1}{2} - \frac{1}{3} \right] - \frac{11}{54} \qquad \text{(II – 15)}$$

For solving equation II – 13, the discriminant function U for the polynomial has to be determined as:

$$f(U) = U^2 - Xo.U - \frac{P}{3} \qquad \text{(II – 16)}$$

This equation has two square roots (V and T), these are:

$$V + T = Xo \qquad \text{(II – 17)}$$

$$V.T = -\frac{P}{3} \qquad \text{(II – 18)}$$

Substituting equation II – 7 in equation II – 13, we get:

$$(V + T)^3 + P (V + T) - 2.R = 0 \qquad\qquad\qquad\qquad\qquad\qquad (\text{II} - 19)$$

$$V^3 + T^3 + (3VT + P) (V + T) - 2.R = 0 \qquad\qquad\qquad\qquad (\text{II} - 20)$$

$3VT + P = 0$ from Equation II – 18,

accordingly, $V^3 + T^3 = 2.4$ \qquad\qquad\qquad\qquad\qquad\qquad\qquad\qquad $(\text{II} - 21)$

Also from equation II – 18, we get:

$$V^3 . T^3 = -\frac{P^3}{27} \qquad\qquad\qquad\qquad\qquad\qquad\qquad\qquad (\text{II} - 22)$$

Equations II – 21 and II – 22 indicate that, V^3 and T^3 are the roots for the equation:

$$Z^2 - 2RZ - \frac{P^3}{27} = 0 \qquad\qquad\qquad\qquad\qquad\qquad\qquad (\text{II} - 23)$$

Solving this equation gives:

$$Z = R \pm \sqrt{R^2 + \frac{P^3}{27}} \qquad\qquad\qquad\qquad\qquad\qquad\qquad (\text{II} - 24)$$

then:

$$V = \sqrt[3]{R + \sqrt{R^2 + \frac{P^3}{27}}} \qquad\qquad\qquad\qquad\qquad\qquad\qquad (\text{II} - 25)$$

$$T = - \sqrt[3]{\left| R - \sqrt{R^2 + \frac{P^3}{27}} \right|} \qquad\qquad\qquad\qquad\qquad\qquad (\text{II} - 26)$$

Equations II – 25 and II – 26 can be written as:

$$V = \sqrt[3]{R + \sqrt{U}} \qquad\qquad\qquad\qquad\qquad\qquad\qquad\qquad (\text{II} - 27)$$

$$T = - \sqrt[3]{\left| R - \sqrt{U} \right|} \qquad\qquad\qquad\qquad\qquad\qquad\qquad (\text{II} - 28)$$

where : $U = R^2 + \left(\dfrac{P}{3}\right)^3$

Substituting equation II – 14 in the above equation, we get:

$$U = R^2 + \left(-\frac{4}{9} + \frac{1}{3\Phi sd}\right)^3 \qquad\qquad\qquad\qquad\qquad\qquad (\text{II} - 29)$$

Substituting equations II – 5, II – 6, II – 7 in equation II – 10, we get:

$$Vsh2 = V + T + \frac{2}{3} \qquad\qquad\qquad\qquad\qquad\qquad\qquad\qquad (\text{II} - 30)$$

Substituting equations II – 27 and II – 28 we have:

$$Vsh2 = \sqrt[3]{R + \sqrt{U}} - \sqrt[3]{\left| R - \sqrt{U} \right|} + \frac{2}{3} \qquad\qquad\qquad\qquad (\text{II} - 31)$$

References

Basal, A.M.K. (1994) Well log response as a guide for detecting the hydrocarbon density and saturation, with computed confidence factor. *Ain Shams Science Bulletin,* **32:** 329-352.

Desbrandes, R. (1985) *Encyclopedia of Well Logging.* Gulf Publishing Company. Houston, Texas, p. 584.

de Witte, L. (1950) Relations between resistivities and fluid contents of porous rocks: *Oil and Gas Jour. August,* **24:** 216-222.

El-Heiny, I., Rizk, R. and **Hassan, M.** (1990) Sedimentological model for Abu Madi reservoir sands, Abu Madi Field, Nile Delta, Egypt. *10th Pet. Exploration and Production Conf.,* **2:** 515-551.

Poupon, A., Clavier, C., Dumanoir, J., Gaymard, R. and **Misk, A.** (1970) Log Analysis of sand-shale sequences – A systematic approach: *Jour. Pet. Tech., July,* pp. 867-874.

——— **Loy, M.E.** and **Tixer, M.P.** (1954) A contribution to electrical log interpretation in shaly sands. *Jour. Pet. Tech., June,* pp. 1795-1804.

Schlumberger (1972) *Log Interpretation,Volume I – Principles.*

——— (1974) *Log Interpretation, Volume II – Applications*

Serra, O. (1986) *Fundamentals of Well Log Interpretations, Volume II. Developments in Petroleum Science.* Elsevier Publ. Co., Amsterdam, pp. 1795-1804.

Simandoux, P . (1963) Measures dielectriques en milieu poreux, application a measure des saturations en eau, étude du comportement des massifs argileux. *Revue de L'Institut Français du Petrole. Supplementary Issue,* pp. 193-216.

معالجـة تحليليـة لتوقيـع النيتـرون والكثافـة المتقاطـع للخـزانات الرمليـة الطفيليـة

أحمد محمد كمال بصل

قسم الجيولوجيا ، كلية علوم دمياط ، جامعة المنصورة

دميـــــاط – جمهورية مصر العربية

المستخلص .   إن التوقيع البياني المتقاطع لبيانات النيترون – الكثافة تمثل الأساس لتحليل خزانات الرمل الطفيلية وتندرج تحت برنامج « ساراباند » . وفي هذا البحث تم استنباط المعادلات الرياضية للحصول على النسب الحجمية للثلاث أنواع من الطفلة (المتوازي والتركيبي والمتنشر) . ويتضمن ذلك تتابع من الحسابات تشمل المسامية بجانب تطبيق نماذج الطفلة الكلية والمتوازية والمتنشرة وذلك لحـساب نسب التـشبع بالماء . أيضًا تمت مـعـالجـة تأثيـر وجـود الهيدروكربونات الخفيفة (الغازات) في هذه الدراسة .

اعتمدت التقنية المقدمة على استخدام قياسات النيترون والكثافة أساسًا لتقييم حجم الطفلة وذلك يـؤدي إلى تجنب الاعتماد على قياسات أشعة جاما حيث إنها قد تتأثر بمعادن مشعة أخرى غير الطفلة فيحدث خلط في النتائج .

لتطبيق تلك المعالجة اختيرت بيانات تسجيلات الآبار تمثل متكون أبو ماضي (رمـال المسـتـوى الثالث) في بئري شـرق بلطيم-١ والقرعـة-٢ (دلتـا النيل) بالإضافة إلى رمال متكون الوقار لبئر بورفؤاد بحري-٣ (شمـال سيناء) . وقد أوضحت النتائج التي تم الحصول عليها إن الطفلة من النوع التركيبي والمتوازي هي السائدة في حالة رمال المستوى الثالث في متكون أبو ماضي . ولذلك تعتبر المعادلة المبسطة للطفلة المتوازية هي الأنسب لحـساب نسب التشبع بالماء في هذه الحالة . وعلى الجانب الآخر احتوت رمال الوقار في بئر بورفؤاد بحري-٣ على الثـلاث أنواع المخـتـلفـة من الطفلة ولذا فـإن نموذج الطفلة الكليـة هـو الأنسب لحـساب نسب التـشبع بالماء في هذه الحـالة . وقـد أيدت نتـائج تاريخ الإنتـاج وبيانات اختبارات الحفر الجزئي (DST) النتائج التي تم التوصل إليها .